



## Distinct structural transitions of chromatin topological domains correlate with coordinated hormone-induced gene regulation

François Le Dily, Davide Baù, Andy Pohl, et al.

*Genes Dev.* 2014 28: 2151-2162

Access the most recent version at doi:[10.1101/gad.241422.114](https://doi.org/10.1101/gad.241422.114)

---

### Supplemental Material

<http://genesdev.cshlp.org/content/suppl/2014/09/29/28.19.2151.DC1.html>

### References

This article cites 45 articles, 15 of which can be accessed free at:  
<http://genesdev.cshlp.org/content/28/19/2151.full.html#ref-list-1>

### Creative Commons License

This article is distributed exclusively by Cold Spring Harbor Laboratory Press for the first six months after the full-issue publication date (see <http://genesdev.cshlp.org/site/misc/terms.xhtml>). After six months, it is available under a Creative Commons License (Attribution-NonCommercial 4.0 International), as described at <http://creativecommons.org/licenses/by-nc/4.0/>.

### Email Alerting Service

Receive free email alerts when new articles cite this article - sign up in the box at the top right corner of the article or [click here](#).

---

**Exiqon Grant  
Program 2014**

Accelerate your RNA discoveries  
with a grant from Exiqon

**EXIQON**

---

To subscribe to *Genes & Development* go to:  
<http://genesdev.cshlp.org/subscriptions>

---

# Distinct structural transitions of chromatin topological domains correlate with coordinated hormone-induced gene regulation

François Le Dily,<sup>1,2,3</sup> Davide Baù,<sup>1,3</sup> Andy Pohl,<sup>1,2</sup> Guillermo P. Vicent,<sup>1,2</sup> François Serra,<sup>1,3</sup> Daniel Soronellas,<sup>1,2</sup> Giancarlo Castellano,<sup>1,2,4</sup> Roni H.G. Wright,<sup>1,2</sup> Cecilia Ballare,<sup>1,2</sup> Guillaume Fillion,<sup>1,2</sup> Marc A. Marti-Renom,<sup>1,3,5</sup> and Miguel Beato<sup>1,2</sup>

<sup>1</sup>Gene Regulacion, Stem Cells, and Cancer Program, Centre de Regulació Genòmica (CRG), 08003 Barcelona, Spain; <sup>2</sup>Universitat Pompeu Fabra (UPF), 08002 Barcelona, Spain; <sup>3</sup>Genome Biology Group, Centre Nacional d'Anàlisi Genòmica (CNAG), 08028 Barcelona, Spain; <sup>4</sup>Hospital Clínic, Universitat de Barcelona, 08036 Barcelona, Spain; <sup>5</sup>Institució Catalana de Recerca i Estudis Avançats (ICREA), 08010 Barcelona, Spain

The human genome is segmented into topologically associating domains (TADs), but the role of this conserved organization during transient changes in gene expression is not known. Here we describe the distribution of progesterin-induced chromatin modifications and changes in transcriptional activity over TADs in T47D breast cancer cells. Using ChIP-seq (chromatin immunoprecipitation combined with high-throughput sequencing), Hi-C (chromosome capture followed by high-throughput sequencing), and three-dimensional (3D) modeling techniques, we found that the borders of the ~2000 TADs in these cells are largely maintained after hormone treatment and that up to 20% of the TADs could be considered as discrete regulatory units where the majority of the genes are either transcriptionally activated or repressed in a coordinated fashion. The epigenetic signatures of the TADs are homogeneously modified by hormones in correlation with the transcriptional changes. Hormone-induced changes in gene activity and chromatin remodeling are accompanied by differential structural changes for activated and repressed TADs, as reflected by specific and opposite changes in the strength of intra-TAD interactions within responsive TADs. Indeed, 3D modeling of the Hi-C data suggested that the structure of TADs was modified upon treatment. The differential responses of TADs to progesterins and estrogens suggest that TADs could function as “regulons” to enable spatially proximal genes to be coordinately transcribed in response to hormones.

[*Keywords:* three-dimensional structure of the genome; gene expression; Hi-C; TADs; transcriptional regulation; epigenetic landscape; progesterone receptor]

Supplemental material is available for this article.

Received March 12, 2014; revised version accepted August 29, 2014.

The three-dimensional (3D) organization of the genome within the cell nucleus is nonrandom and might contribute to cell-specific gene expression. High-throughput chromosome conformation capture (3C)-derived (Dekker et al. 2002) methods have revealed that chromosome territories are organized in at least two chromatin compartments—one open and one closed—that tend to be spatially segregated depending on their transcriptional activity (Lieberman-Aiden et al. 2009). At a finer level of organization, some functionally related genes have been shown to be brought close in space to be transcribed in a correlated fashion during cell differentiation. These

genes, which can be located on different chromosomes, are organized in spatial clusters and preferentially transcribed in the same “factories” (Osborne et al. 2004, 2007; Cavalli 2007). Whether such mechanisms participate in transient modifications of the transcription rate in differentiated cells responding to external cues is still unclear (Fullwood et al. 2009; Kocanova et al. 2010; Hakim et al. 2011). Transient regulation of gene expression at the transcription level depends on the establishment of regulatory

Corresponding authors: [miguel.beato@crg.es](mailto:miguel.beato@crg.es), [mmarti@pcb.ub.cat](mailto:mmarti@pcb.ub.cat)  
Article is online at <http://www.genesdev.org/cgi/doi/10.1101/gad.241422.114>.

© 2014 Le Dily et al. This article is distributed exclusively by Cold Spring Harbor Laboratory Press for the first six months after the full-issue publication date (see <http://genesdev.cshlp.org/site/misc/terms.xhtml>). After six months, it is available under a Creative Commons License (Attribution-NonCommercial 4.0 International), as described at <http://creativecommons.org/licenses/by-nc/4.0/>.

Le Dily et al.

loops between regulatory enhancers and the promoter of responsive genes. Recent studies have demonstrated that these networks of interactions and the precise molecular mechanisms were more complex than initially thought (Shen et al. 2012; Thurman et al. 2012). Notably, a recent study showed that TNF-responsive gene promoters are unexpectedly found juxtaposed to TNF-responsive regulatory elements prior to stimulation, supporting the importance of the 3D chromatin landscape in cell-specific gene regulation (Jin et al. 2013).

Recently, an intermediate level of partitioning of the chromosomes in so-called topologically associating domains (TADs) has been revealed (Dixon et al. 2012; Hou et al. 2012; Nora et al. 2012; Sexton et al. 2012). Changes in the levels of expression of genes appeared to be correlated within TADs during cell differentiation (Nora et al. 2012), potentially by topologically constraining enhancer or silencer activity (Symmons et al. 2014). However, whether the spatial structure of TADs plays a role in regulating the transient response to external signals in terminally differentiated cells remains mainly hypothetical (Nora et al. 2013). We addressed this issue using the T47D cell line—a progesterone receptor (PR)-positive and estrogen receptor (ER)-positive breast cancer cell line (Truss et al. 1995)—that responds to steroids with transient changes in gene expression. We studied the relationship between hormone-regulated changes in transcription, chromatin structure, epigenetic marks, and the 3D structure of TADs. We know that the progestin (Pg)-activated PR cross-talks with kinase signaling networks to modify chromatin and regulate the transcription rate of thousands of target genes by either activation or repression (Migliaccio et al. 1998; Vicent et al. 2006, 2011; Wright et al. 2012). Using RNA-seq (RNA sequencing), ChIP-seq (chromatin immunoprecipitation combined with high-throughput sequencing), Hi-C (chromosome capture followed by high-throughput sequencing), and 3D modeling, we confirmed that the T47D genome is organized into ~2000 TADs whose borders are largely stable upon hormone treatment. Around 20% of TADs showed a general biased transcriptional response to Pg and/or estradiol (E<sub>2</sub>), with topological segregation of hormone-induced stimulation and repression of gene expression. Moreover, Pg treatment induced large-scale modifications of TAD chromatin structure, which correlated with changes in spatial organization within the responsive TADs. Integrative 3D modeling indeed suggested that responsive TADs were specifically structurally modified upon treatment. Such structural changes were correlated with differential changes in chromatin and gene expression, suggesting a link between the structure of TADs and their activity. Altogether, our results generalize the proposed hypothesis of TADs functioning as “regulons” for transcription (Nora et al. 2012).

## Results

### *Characterization of TADs in T47D cells*

To test whether the spatial organization of the genome into TADs is important for the response of T47D breast

cancer cells to Pg, we generated Hi-C libraries of cells synchronized in G<sub>0</sub>/G<sub>1</sub> and treated or not with Pg for 60 min, when most of the Pg-induced chromatin modifications that we described previously already occurred (Vicent et al. 2008; Wright et al. 2012; Ballare et al. 2013). In order to minimize artifacts linked to the biased genomic distribution of restriction enzymes (Yaffe and Tanay 2011; Imakaev et al. 2012), we generated biological replicates of Pg treatment using, independently, HindIII and NcoI (giving a total of 174,278,292 and 169,171,077 pairs of interacting fragments, respectively, for –Pg and +Pg cells, respectively) (see the Supplemental Material; Supplemental Table 1). Contact matrices at various scales showed that despite the chromosomal rearrangements in the T47D cell line (Supplemental Fig. 1A), the genome conserves the general principles of organization described for other cell types—notably the segmentation of chromosomes into TADs (Fig. 1A). The contact maps obtained with HindIII and NcoI yielded similar TAD borders (Fig. 1A). These data sets were therefore pooled to robustly define the position of TADs using a novel algorithm based on a change point detection approach (see Supplemental Material; Supplemental Fig. 1B). By testing different resolutions, we achieved the most robust identification of TAD boundaries at 100 kb, at which we identified 2031 TADs with a median size of ~1 Mb (Supplemental Fig. 1C,D). These were organized as described in other cell types (Dixon et al. 2012; Hou et al. 2012; Nora et al. 2012; Sexton et al. 2012), with enrichment of genes and active epigenetic marks near their borders (Supplemental Fig. 2A–C). Despite this enrichment, in median, we observed that genes were located at >200 kb from the TAD borders (Supplemental Fig. 2D).

To investigate the chromatin states of the identified TADs, we analyzed various ChIP-seq experiments performed in this cell line under similar conditions of culture and treatment (Fig. 1B; Supplemental Table 2). We found that histone marks were frequently spread over entire TADs, which suggested that TAD borders delimit large chromatin blocks (Fig. 1B). Epigenetic marks were more homogeneous within than between TADs, and the transitions between high and low levels of the analyzed epigenetic marks occurred preferentially at the borders (Fig. 1B; Supplemental Fig. 3A), suggesting that TAD boundaries can act as a barrier between epigenetic states and that TADs harbor specific epigenetic signatures. To confirm this hypothesis, we calculated pairwise the correlations between the profiles of the combinations of epigenetic marks presented for 100-kb windows. Correlations were higher within TADs than either between TADs or within random genomic domains of similar size obtained by either shifting or inverting the TAD borders from telomeres to centromeres on each chromosomal arm (“same random genomic domains”) (Fig. 1C,D). We thus used the correlation matrices generated above to delimit epigenetic domains according to the combinations of epigenetic marks (see the Supplemental Material; Supplemental Fig. 3B). The borders of such domains overlapped more frequently with the TAD borders than with random segmentations of the genome (Supplemental Fig. 3B),

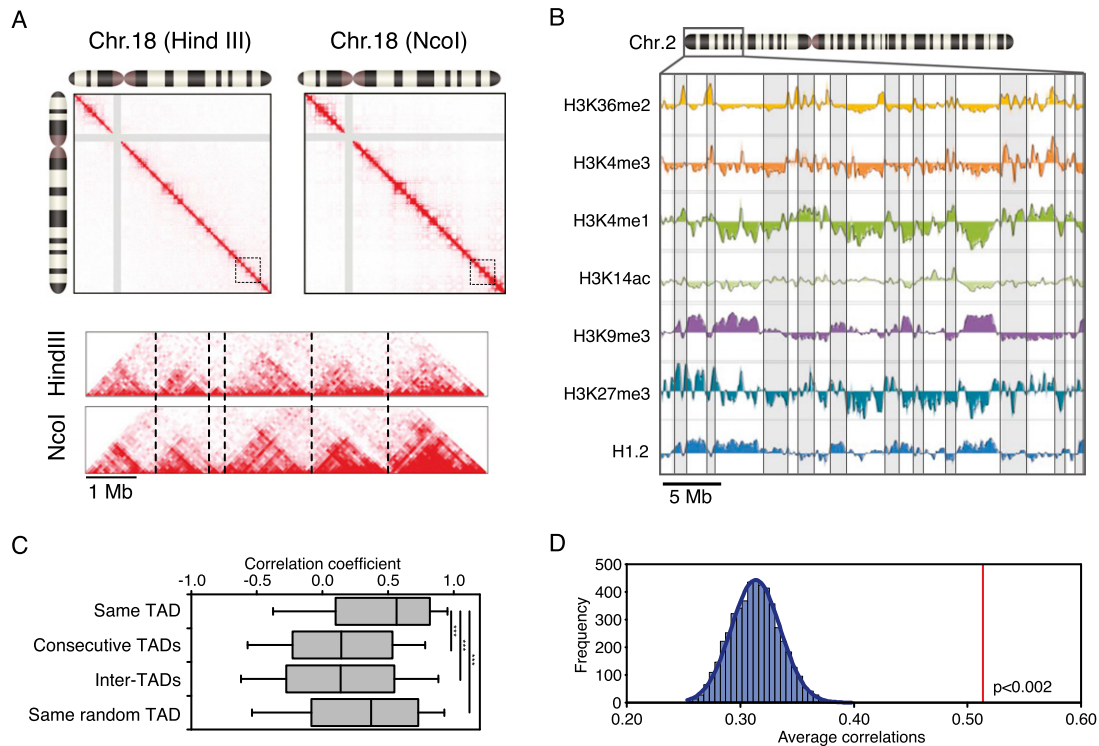


**Figure 1.** Topological chromatin landscapes defined in T47D cells. (A) Hi-C contact matrices of the chromosome 18 obtained using HindIII or NcoI. Both restriction enzymes resulted in detection of similar TAD borders (dashed lines on the rotated magnification). (B) Log<sub>2</sub>-normalized ChIP-seq/input ratio obtained with antibodies against the indicated epigenetic marks over windows of 100 kb on a 30-Mb region of the chromosome 2. (C) Distributions of pairwise correlation coefficients of chromatin profiles between 100-kb chromosomal fractions located within the same TAD, within consecutive or randomly picked TADs (inter-TADs), or in a similar randomly defined domain for the region depicted in B (see the Supplemental Material). (\*\*\*)  $P < 0.001$ ; Mann-Whitney test. (D) Similar analysis was performed genome-wide, and the results were compared with 5000 randomizations of TAD borders (see the Supplemental Material). The histogram shows the distribution of genome-wide averages of the calculated correlation coefficients. The red bar (0.536) corresponds to the average correlation coefficients calculated for the real positions of the borders ( $P < 0.002$ ).

supporting the concept of topological segregation of regions of the genome with distinct chromatin signatures. Together, these observations indicate that the TAD borders that we defined in T47D delimit epigenetic domains and that transitions between domains of different states occur preferentially at the boundaries between TADs, which confirms previous studies (Dixon et al. 2012; Hou et al. 2012; Nora et al. 2012; Sexton et al. 2012).

#### TADs respond as units to the hormone

We observed that ~80% of TAD borders detected without Pg treatment remained similarly positioned after Pg stimulation (the other 12% of the borders were found shifted by only 100 kb) (Fig. 2A). TADs that showed nonconserved borders did not show any specificity regarding their response to the hormone, suggesting that those changes were not linked to the treatment but rather corresponded to stochastic or technical variability. Thus, the T47D genome is organized in TADs that do not significantly change boundaries in response to Pg.

We previously showed that gene regulation by Pg involves a complex interaction of hormone receptors with kinase signaling pathways and chromatin remodeling

enzymes to modulate the transcriptional output (Vicent et al. 2008; Wright et al. 2012). Here, we observed that the Pg-induced modifications of chromatin marks could occur over large genomic domains (Fig. 2B). Although these modifications of chromatin states could spread over consecutive TADs or be more local within TADs (Fig. 2B), the transitions between divergent chromatin changes occurred more frequently at the TAD borders (Fig. 2B; Supplemental Fig. 3C). Importantly, the combinations of Pg-induced changes were more homogeneous within TADs than either between TADs or within random genomic domains of similar size (Fig. 2C,D; Supplemental Fig. 3D), indicating that differential Pg-induced changes in chromatin mark levels are restrained within some TADs. Overall, our results indicate that TADs could act as epigenetic domains, the chromatin of which can be coordinately modified in response to external cues.

The observations above suggested that TADs could topologically constrain transient Pg-induced changes in gene expression. To explore this hypothesis, we performed RNA-seq experiments in T47D treated or not with Pg for 6 h (Supplemental Table 3). We observed that a limited but significant number of TADs have the majority of their genes either activated or repressed by the hormone (examples

Le Dily et al.

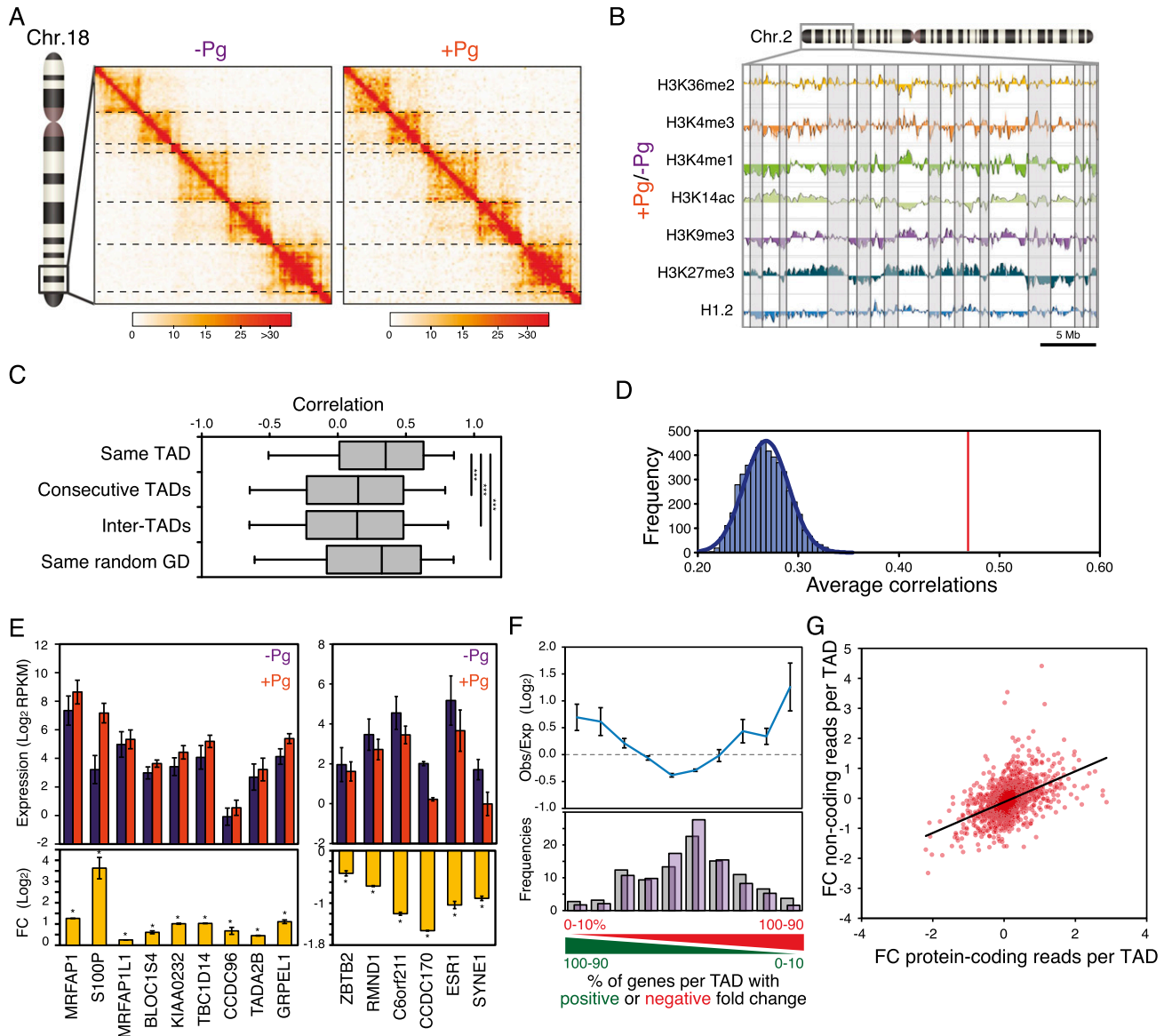


**Figure 2.** TAD chromatin and activity are coordinately modified upon hormone stimulation. (A) Chromatin interaction maps of a 10-Mb region of the chromosome 18 before (-Pg) and after (+Pg) 1 h of Pg treatment (determined TAD borders are depicted by the horizontal dashed lines). (B) Log<sub>2</sub> ratio of normalized ChIP-seq signals +Pg/-Pg treatment over a 30-Mb region of the chromosome 2. (C) Distributions of pairwise correlation coefficients of Pg-induced chromatin profile changes between 100-kb chromosomal fractions located within the same TAD, within consecutive or randomly picked TADs (inter-TADs), or in a similar randomly defined genomic domain (GD) for the region depicted in B (see the Supplemental Material). (\*\*\*)  $P < 0.001$ ; Mann-Whitney test. (D) Similar analysis was performed genome-wide, and the results were compared with 5000 randomizations of TAD borders (see the Supplemental Material). The histogram shows the distribution of genome-wide averages of the calculated correlation coefficients. The red bar (0.466) corresponds to the average correlation coefficients calculated for the real positions of the borders ( $P < 0.002$ ). (E) Examples of TADs with biased coordinated response to hormone—either activation (TAD 469, Chr.4: 6,600,000–7,100,000) (left) or repression (TAD 821, Chr.6: 151,700,000–152,700,000) (right). (Top panels) Expression levels [reads per kilobase per million mapped reads [RPKM]] of all consecutive protein-coding genes within those TADs as determined by RNA-seq (average  $\pm$  standard error of the mean) before (-Pg) or after (+Pg) 6 h of treatment with Pg. The bottom panels show the log<sub>2</sub> ratio (+Pg/-Pg) of expression of the individual genes obtained after 6 h of treatment with Pg. (\*)  $P$ -value  $< 0.05$ ; FDR  $< 0.01$ . (F, top panel) Ratio of observed versus expected frequencies of TADs with distinct proportions of genes with positive or negative Pg-induced FC; FC  $> 1$  or FC  $< 1$ . (Bottom panel) Histogram of the frequencies of TADs for the observed (gray) or randomized (purple) position of genes. (G) Scatter plot showing the correlation between Pg-induced changes of expression of the pool of protein-coding versus non-protein-coding reads per TAD ( $R = 0.488$ ;  $P < 0.001$ ).

are shown in Fig. 2E). Furthermore, in addition to the thousands of genes significantly regulated by Pg ( $P$ -value  $< 0.05$ , false discovery rate [FDR]  $< 0.01$ , threshold = 1.5),

we observed a nonrandom distribution of divergent Pg-induced modifications of gene expression through the genome, with stretches of genes whose expression either

slightly increases or decreases upon treatment. To determine whether it reflected coordinated changes of expression within TADs, we calculated the percentage of genes per TAD with a positive or negative fold change (FC) after Pg treatment. In this analysis, 410 TADs with four or more genes (i.e., 20% of all TADs) were found to harbor at least 75% of their genes changing expression in a similar direction upon hormone (Fig. 2F), representing a significant enrichment compared with the expected frequencies obtained after robust randomizations of the gene positions that conserved an equivalent basal level of gene expression for each TAD ( $P < 0.0001$ ) (Fig. 2F; see Supplemental Material). In addition, independent analysis of the Pg-induced changes in RNA-seq reads for protein-coding and non-protein-coding regions located within the same TAD revealed that their changes of expression were significantly correlated (Pearson  $R = 0.48$ ;  $P < 0.001$ ) (Fig. 2G; see the Supplemental Material; Supplemental Fig. 4A,B). Together, those results indicate that genes with an opposite response to Pg tend to be segregated in distinct TADs and that some TADs can be affected by either a global repression or stimulation of the expression of the genes that they contain.

To characterize, in a nonbiased way, TADs according to their activation or repression by Pg, we ranked TADs containing more than three protein-coding genes according to their global Pg-induced changes of expression (using the average +Pg/−Pg ratio of the sum of normalized reads per TAD) (see Supplemental Fig. 5A; Supplemental Material) and studied the 100 top and bottom TADs (further mentioned as Pg-activated or Pg-repressed TADs, respectively). We compared them with the remaining TADs, referred to by default as “other TADs,” although they include some TADs presenting a biased response to hormones to a lower extent than the top ones (Fig. 3A). Due to the time required for transcript accumulation or degradation, few genes could be found modified significantly by Pg after only 1 h of treatment (Supplemental Fig. 5B). Nevertheless, coherent activity changes were already observed after 1 h of Pg treatment within the activated and repressed TADs (Supplemental Fig. 5C). Activated and repressed TADs contain ~15% of the significantly up-regulated and down-regulated genes, respectively, although they only carry ~5% of all genes. On average, significantly up-regulated genes represented 32% of the genes within activated TADs. Conversely, down-regulated genes represented 18% of the genes within repressed TADs, while, in nonresponsive TADs, up-regulated and down-regulated genes represent 10% and 6% of the genes, respectively. In these top and bottom TADs, the expression levels of most protein-coding genes (~70%) were modified according to the global TAD response (Fig. 3B), supporting the hypothesis of coordinated response. These changes were irrespective of the basal expression levels of genes within activated or repressed TADs (Supplemental Fig. 5D), although responsive TADs showed a lower gene density (Supplemental Fig. 5E). More generally, significantly up-regulated and down-regulated genes were found enriched in TADs in which the global response to hormone was biased toward activation or repression, respectively: Twenty-three

percent of the significant Pg-up-regulated genes were found in TADs in which >75% of the genes were affected positively by the hormone; conversely, 20% of the down-regulated genes were located within TADs biased toward repression. This confirms that some TADs classified as others are also biased in their response to hormone. Around 45% of TADs classified as activated and repressed showed at least 75% of their protein-coding genes with signs of Pg-induced changes coherent with the response at the TAD scale (Fig. 3C). In addition, the transcribed non-coding regions responded to Pg in the same direction as the protein-coding genes (Fig. 3D), suggesting that a global coordinated response of genes within responsive TADs is a relatively frequent event.

We next tested the TAD response to a different steroid hormone; namely, E2. In T47D cells, although fewer genes responded significantly to E2 than to Pg (Supplemental Fig. 5B), the response was not random throughout the genome. We selected the 100 TADs maximally activated or repressed by E2 and analyzed their overlap with the Pg-responsive ones. Most of the TADs showed a differential response to the two hormones (Fig. 3E). Only 17 of the Pg-activated TADs showed activation upon E2, and 38 TADs were repressed by both hormones (Fig. 3E; Supplemental Fig. 5F; for examples, see Supplemental Fig. 6A–C), while 18 TADs showed an opposite response to the two hormones (Fig. 3E, F). These results confirm that some TADs respond as a unit to external stimuli and show that the response can be different depending on the nature of the stimulus.

#### *Changes in expression correlate with PR-induced changes on chromatin and global reorganization of intra-TAD interactions*

The changes in TAD transcription were accompanied by coherent changes in the levels of epigenetic marks and structural chromatin proteins detected at the TAD level (Fig. 4A). Activated TADs showed relatively increased levels of active marks (H3K36me2 and H3K4me3), whereas repressive marks (H3K9me3 and H3K27me3) were accumulated within repressed TADs (Fig. 4A). DNase I sensitivity was increased in activated TADs, suggesting that those TADs were submitted to an opening of the chromatin fiber and were becoming more permissive for transcription. Conversely, repressed TADs showed increases in H1 and HP1 levels together with H2A, suggesting that the chromatin of those TADs was less permissive and more compact after Pg, as indicated by the higher protection upon MNase digestion (Fig. 4A). No coherent changes were observed in nonregulated TADs.

Those changes, consistent with our previous observations made at the gene level (Vicent et al. 2008; Wright et al. 2012; Ballare et al. 2013), occur during the first 60 min after hormone exposure, are necessary for the changes in transcription, and could impact on the TAD structure. We therefore measured the relative Pg-induced changes of intra-TAD interactions in the different types of TADs. Strikingly, activated and repressed TADs showed an opposite redistribution of the interactions emerging from

Le Dily et al.

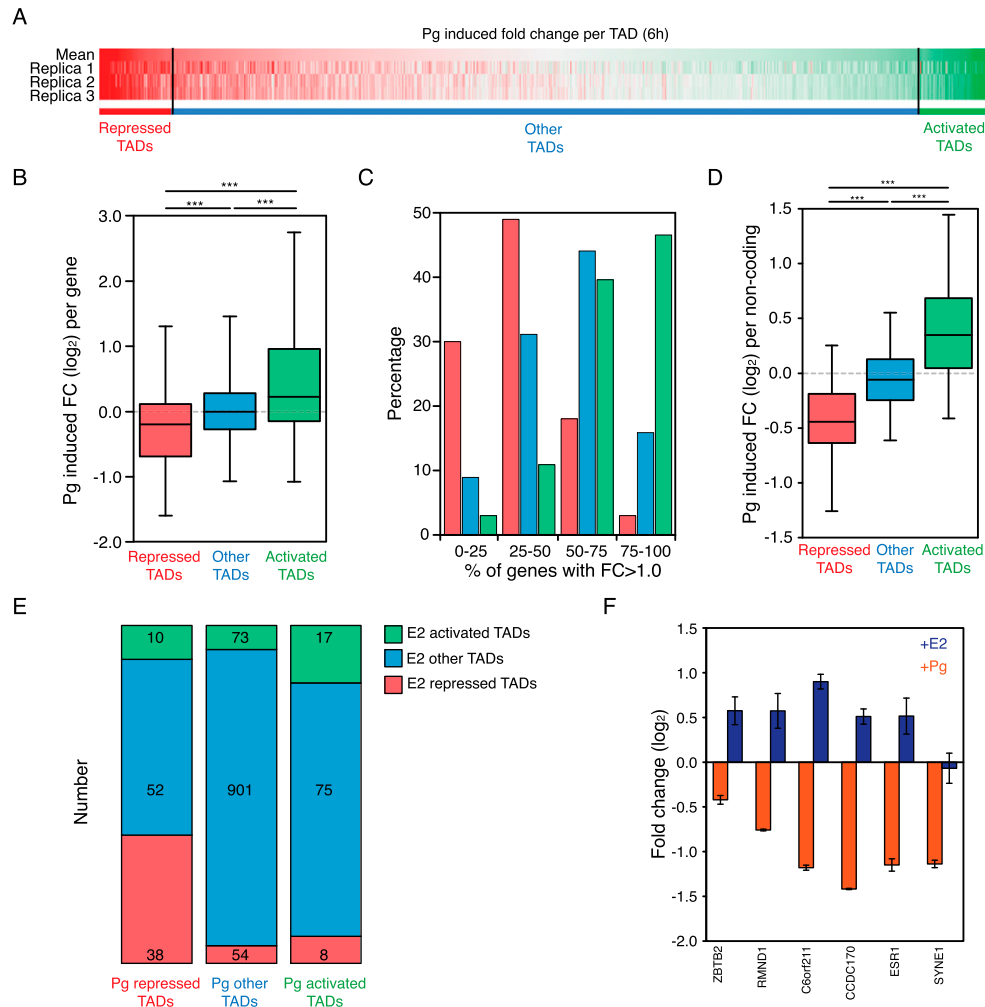


**Figure 3.** TADs respond as units to the hormone in a stimulus-specific manner. (A) Heat map of TADs ranked according to their average global changes of expression after 6 h of treatment with Pg (ratio of the sum of sequencing depth-normalized RNA-seq reads per TADs in three biological replicates of RNA-seq). The 100 top and bottom TADs were classified as Pg-repressed or Pg-activated TADs. (B) Distributions of Pg-induced FCs in the expression of protein-coding genes after 6 h of treatment with Pg in the types of TADs classified above according to the changes detected in the global TAD level. (C) Histograms show the distributions of the percentages of TADs of each type ([green] activated; [red] repressed; [blue] others) that contains the indicated proportions of genes, with positive FC indicated on the X-axis. (D) Distributions of Pg-induced FCs of expression for regions that do not contain any annotated protein-coding gene for the different types of TADs. (E) TADs were ranked according to their global changes of expression upon E2 treatment, and the 100 top and bottom TADs were classified as E2-activated and E2-repressed, as for Pg. (Bottom) The graphic shows the fractions of TADs with a given E2 response classified according to their Pg response. (F) Example of a TAD (TAD 821, Chr.6: 151,700,000–152,700,000) with an opposite response to Pg (orange; same as in Fig. 2E) or E2 (purple). The ratio (log<sub>2</sub>) of the expression of individual genes obtained after 6 h of treatment with hormone is represented. (B,D) Box plot whiskers correspond to the fifth and 95th percentiles. (\*\*\*)  $P < 0.001$  (Bonferroni-corrected Mann-Whitney test).

the domain, with the repressed ones more likely to lose intra-TAD interactions than the rest of the TADs (Fig. 4B). This correlation between changes in transcriptional activity and relative changes in interaction frequencies was observed in the two Hi-C data sets (HindIII and NcoI), supporting their Pg dependence (Supplemental Fig. 7A,B). Thus, Pg induced changes in the topology of responsive domains in addition to the changes in chromatin. To assess whether the activated PR drives these chromatin and structural modifications, we analyzed the distribution of PR-binding sites (PRBSs) as determined by ChIP-seq after 5, 30, 60, and 360 min of Pg treatment (Fig. 4C). PRBS

density at any time point was higher in activated TADs than in other TADs. At early time points, PRBS density was also higher in repressed TADs than in nonresponsive TADs, suggesting that functional binding of PR is the initial step leading to the chromatin and structural rearrangements of TADs (an example of PRBS density within responsive TADs is shown in Supplemental Fig. 6D). Genome-wide, both the number and density of PRBSs per TAD were correlated with the extent of chromatin remodeling, homogeneity, and strength of the transcriptional response (Fig. 4D). PR binding within TADs correlates with the extent of chromatin opening as reflected by DNase I

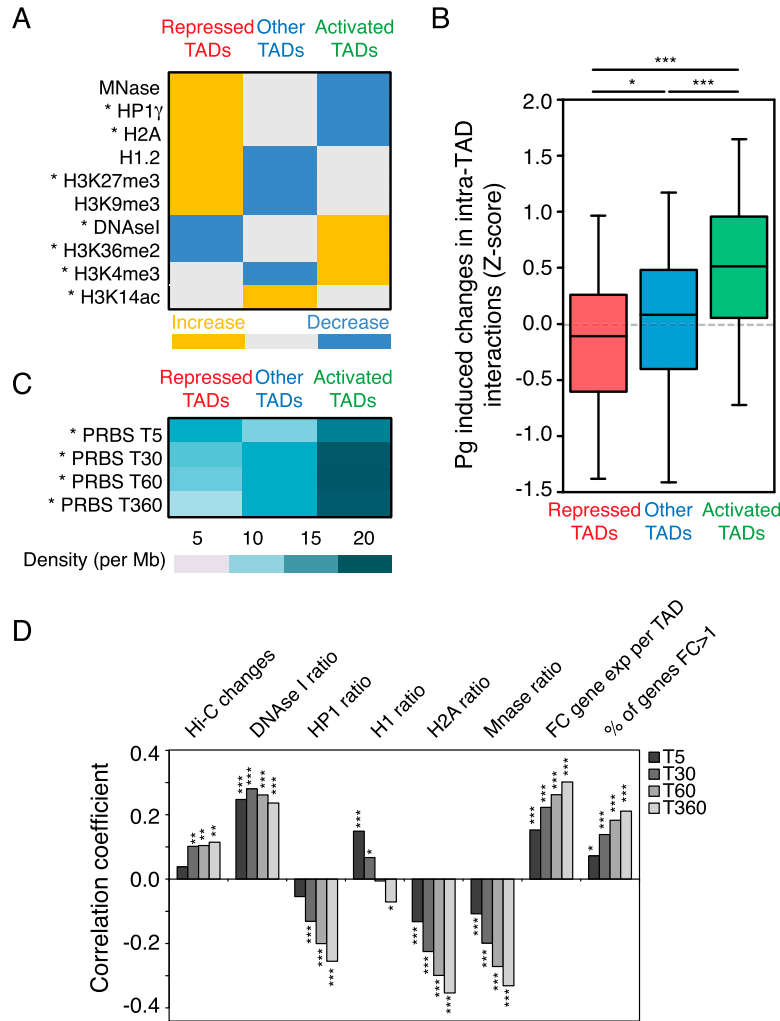


**Figure 4.** Changes in expression correlate with PR-induced changes in chromatin and reorganization of intra-TAD interactions. (A) Heat map of the median of the ratio per TAD of normalized ChIP-seq signals with or without treatment for the different classes of TADs ([blue] relative Pg-induced decreases; [orange] Pg-induced increases). (\*) Different populations with  $P < 0.05$  (Bonferroni-corrected Mann-Whitney test). (B) Distributions of the relative changes for intra-TAD interactions after 1 h of treatment with Pg in the three types of TADs (Z-scores of normalized intra-TAD interactions +Pg/−Pg). Box plot whiskers correspond to fifth and 95th percentiles. (\*\*\*)  $P < 0.001$ ; (\*)  $P < 0.05$  (Bonferroni-corrected Mann-Whitney test). (C) Distributions of the density (per megabase) of PR-binding sites (PRBSs) after 5, 30, 60, and 360 min of treatment with Pg according to the TAD categories. (\*) Different populations with  $P < 0.05$  (Bonferroni-corrected Mann-Whitney test). (D) Histograms correspond to the Pearson coefficients of the correlation between the density of PRBSs at different times per TAD and the parameters listed. (\*\*\*)  $P < 0.001$ ; (\*\*\*)  $P < 0.01$ ; (\*)  $P < 0.05$ .

sensitivity and MNase protection, reflecting its dominant role in activated TADs. At 5 min, however, PR binding correlated with H1 loading, reflecting its role in repressed TADs. In addition, PRBS density also correlated with the changes in interactions of responsive TADs (Fig. 4D).

To interpret the Pg changes in interactions in terms of a spatial structure–function relationship, we generated 3D models of 61 genomic regions of the T47D genome harboring 121 TADs with at least four genes, of which 14 and 28 were classified above as transcriptionally repressed and activated by Pg, respectively (Supplemental Table 4). Models were built based on our Hi-C data sets using the integrative modeling platform (IMP) (Russell et al. 2012) as previously described (Supplemental Material; Bau and Marti-Renom 2012). We pooled the normalized Hi-C data sets obtained with NcoI and HindIII and used the interaction matrices at a resolution of 20 kb, resulting in  $\sim 50$  interacting particles per modeled TAD. To validate the modeling approach, we compared 3D models obtained for a region of chromosome 1 with the results of FISH experiments on the same region. We used five fluorescent probes located within the same TAD and/or near the borders (Supplemental Fig. 7C). As previously described

(Mateos-Langerak et al. 2009), the spatial distances measured in situ and in the models increased with the genomic distances (Supplemental Fig. 7D,E). Despite scale differences, the distances calculated from the 3D models correlated with the 3D FISH distances ( $R = 0.94$ ) (Supplemental Fig. 7C). We built 2000 models for each of the 61 genomic regions and analyzed the top 1000 models (i.e., with the lowest IMP objective function).

In many cases, the models obtained after hormone exposure could not be superimposed on the ones obtained before treatment (Fig. 5A). Although this variability was also observed for nonresponsive TADs, up to 88% of the Pg-responsive TADs showed structural segregation of the models between conditions, whereas it was the case for only 63% of the nonresponsive TADs. This suggested that responsive TADs could be specifically structurally modified upon hormone exposure (Fig. 5A).

To test whether the structural changes correlated with changes in transcription, we calculated various structural parameters from the models (namely, radius of gyration, accessibility, and chromatin density) (see the Supplemental Material) and correlated the changes of these parameters between conditions to the changes observed on

Le Dily et al.

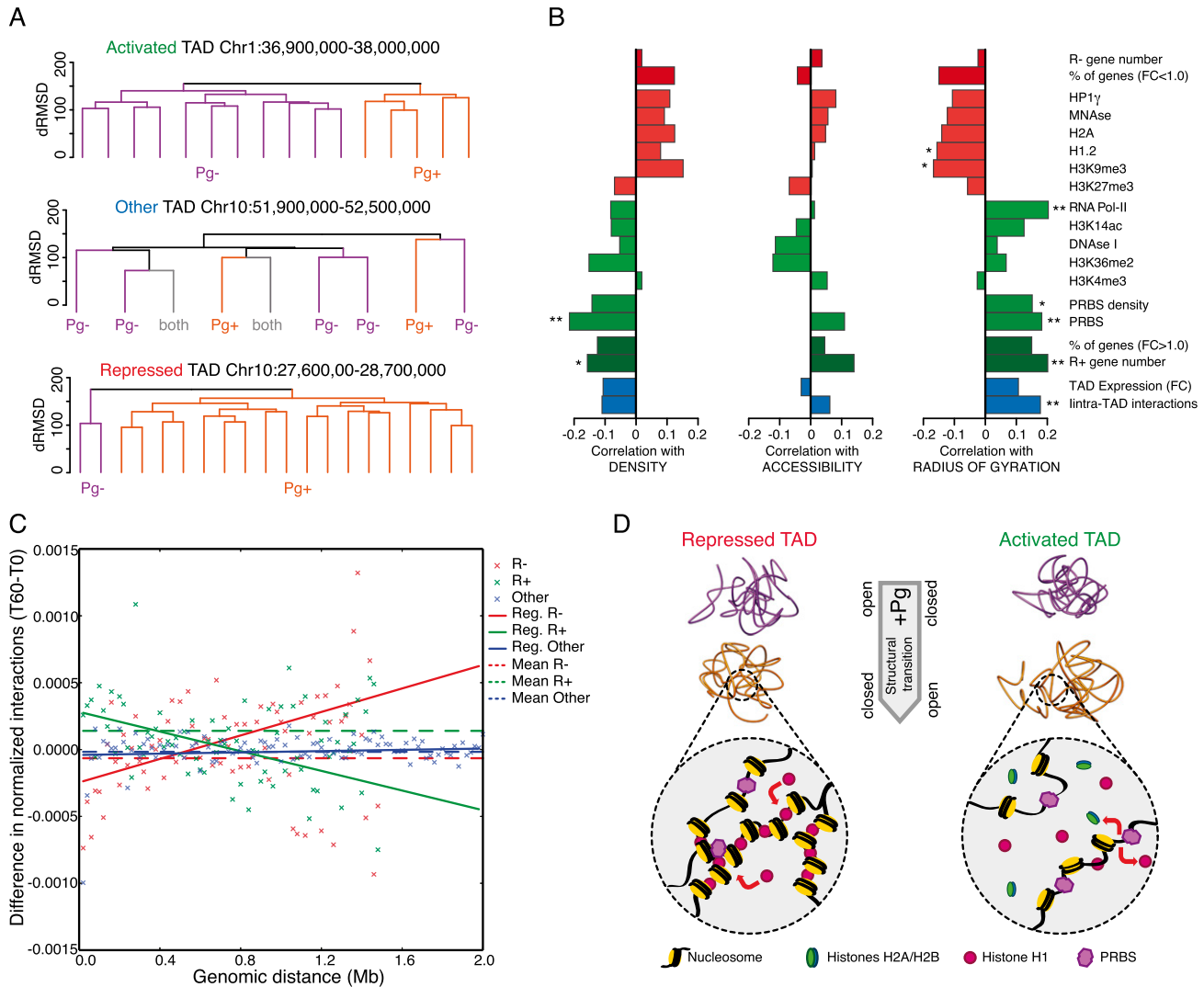


**Figure 5.** Responsive TADs are submitted to distinct structural reorganization upon hormone exposure. (A) Examples of 3D models of activated, “other,” and repressed TADs. Graphs are the dendrograms of the similarities between the resulting structural clusters of all models obtained for the TADs before (–Pg; purple) and after (+Pg; orange) treatment. (B) Histograms show the Pearson correlation coefficients between the Pg-induced changes in the structural parameters derived from the 3D models (density, accessibility, and radius of gyration) and Pg-induced changes in the levels of the chromatin marks listed as well as other features of the TADs: number of significantly up-regulated (R+) or down-regulated (R–) genes, percentage of genes with FC > 1 or FC < 1 per TAD, Pg-induced FC detected at the TAD level (TAD expression FC), number and density of PRBSs per TAD, and Pg-induced changes in intra-TAD interactions. (\*\*) $P < 0.01$ ; (\*) $P < 0.05$ . (C) The plot shows the average differences in interactions induced by Pg between loci of a similar TAD according to the genomic distances that separate them for activated (green), repressed (red), and other TADs (blue). Trend lines for each type of TAD are represented by the plain colored lines. Dashed colored lines show the average Pg-induced differences of interactions determined at the whole TAD level. (D) Model of Pg-induced structural reorganization of responsive TADs: Within activated and repressed TADs, hormone-activated PR bound to chromatin (PRBS) orchestrates distinct reorganization of chromatin in responsive TADs. Those events are accompanied by opposite reorganizations of the TAD structure.

chromatin and gene expression in the corresponding TADs. The changes in radius of gyration were generally negatively correlated with chromatin markers that reflect condensation or transcriptional repression (Fig. 5B), whereas they correlated positively with increased transcriptional activity, as reflected by H3K36me2 and RNA polymerase II recruitment. Changes in the density of chromatin within the models showed the opposite trend (Fig. 5B). Importantly, those changes in structures were

also correlated with the amount of responsive genes harbored by the TADs as well as the number of PRBSs (Fig. 5B). These observations therefore show that in response to hormones and in conjunction with changes on chromatin, the structure of the TADs is modified differentially depending on the strength and direction of transcriptional response. Upon Pg treatment, transcriptionally activated TADs tend to show increases of their radius of gyration and decreases of their internal chromatin density,

whereas repressed TADs show the opposite trend, suggesting changes in their degree of compaction. Unexpectedly, in activated TADs, an increase of the radius of gyration was positively correlated with the relative increase of intra-TAD interactions. To examine whether those observations were reflecting a specific redistribution of the detected Hi-C interactions, we analyzed the changes in interaction induced by Pg with respect to the genomic distance between the interacting loci (Fig. 5C). This analysis confirmed that, overall, intra-TAD interactions increased in activated TADs as compared with repressed TADs (Fig. 5C). However, up-regulated TADs increased their interactions in medium genomic distances (>20 kb up to 200 kb) and decreased their interactions in long genomic distances after hormone treatment. Conversely, down-regulated TADs decreased their interactions in medium genomic distances and increased their interactions in long genomic distances, whereas no specific local redistribution of interactions was seen for other TADs (Fig. 5C). A decrease of distant interactions will result in expanding TADs (up-regulated), while an increase of such interactions will result in compacting TADs (down-regulated) in the 3D models. To analyze the extent of Pg-induced structural changes for individual TADs, we defined a restructuration index (sum of changes in internal interactions, radius of gyration, and accessibility minus changes of chromatin density; highest scores reflect the acquisition of a more decompacted structure). Fifty-five percent of the modeled activated TADs exhibited a high index, and only 17% had a low restructuration index. Conversely, only 25% of the repressed TADs had a high index, suggesting that they were more prone to compact after hormonal treatment. To note, 25% of modeled TADs classified as “others” had a high index of structural changes. Interestingly, those TADs contained a higher percentage of genes positively affected by the hormone, supporting the relationship between structural and transcriptional changes. This indicates that responsive TADs are structurally modified upon treatment in divergent ways. In addition, these observations, together with the changes in chromatin, suggest that activated TADs get a more decondensed structure upon treatment, whereas the repressed TADs become more compacted (Fig. 5D).

## Discussion

Large-scale or genome-wide studies of chromosome conformation by 5C (chromosome conformation capture carbon copy), Hi-C, or TCC (tethered conformation capture) (Dostie et al. 2006; Lieberman-Aiden et al. 2009; Kalthor et al. 2012) revealed that the mammalian genome is organized in a hierarchy of structures in which chromatin globules (Bau et al. 2011) and TADs (Dixon et al. 2012; Nora et al. 2012) are integrated into chromatin compartments (Dekker et al. 2013). We found that in the T47D breast cancer cell line, this high level of genomic organization is conserved, including the partitioning of chromosomes into ~1-Mb-sized TADs. Since it has been proposed that TADs topologically separate chromatin

domains with differential activity during differentiation (Nora et al. 2012), we hypothesized that it could also participate in coordinated gene regulation by constraining the nuclear environment of genes in terminally differentiated cells. The nonrandom organization of genes along eukaryotic chromosomes is well established and plays a role in the coordination of gene expression (Caron et al. 2001). Increasing evidence demonstrates that such coordination of expression might depend on looping-mediated interactions between regulatory elements and gene promoters, which could be located far away in the linear genome sequence (Bau et al. 2011; Sanyal et al. 2012; Jin et al. 2013).

We used the response of a breast cancer cell line to a progesterone analog (Pg) to explore a possible function of TADs in hormonal gene regulation. We confirmed that epigenetic states are more homogeneous within a TAD and that TAD borders frequently prevent the spreading of epigenetic features (Dixon et al. 2012; Hou et al. 2012; Nora et al. 2012; Sexton et al. 2012). Our analysis supports the concept that TADs represent homogeneous epigenetic domains with distinct permissiveness to transcription. RNA-seq analysis demonstrated that Pg target genes are nonrandomly located throughout the genome. Not only are significantly responsive genes enriched in a limited number of TADs, but, more generally, genes differentially affected in response to Pg are frequently segregated in distinct TADs, which therefore could respond as units to the treatment. Indeed, we observed that within some TADs, the majority of the genes were regulated by hormones in a similar direction and that significant hormone-responsive genes were frequently found in such domains.

We also show that changes of gene expression are accompanied by large-scale chromatin modifications and structural transitions of the TADs, supporting the idea that TADs provide a structural base for local coordination of transient gene expression changes in differentiated cells. It is tempting to propose that such a coordinated response depends on the high frequency of self-interactions within the limited space defined by the TAD borders. Stimulus-activated enhancers or silencers would preferentially act on genes located within the same TAD and would influence coordinately their expression in a stochastic way. Such a view is in line with observations made for the ER using a ChIA-PET (chromatin interaction analysis with paired-end tag sequencing) approach (Fullwood et al. 2009) and is supported by the fact that in activated TADs, PRBSs are enriched and correlate with changes in chromatin, redistribution of Hi-C interactions, and structural differences in our 3D models. Similarly, early PR binding is higher in repressed TADs, in conjunction with increased levels of H1 and HPI structural proteins and a relative increase in long-distance intra-TAD interactions.

Interestingly, it appears that some TADs could also respond coordinately to another stimulus (namely, E2) and that, in some cases, a given TAD could respond in an opposite direction to the two hormones. Long-range remodeling of chromatin over megabase-sized domains

Le Dily et al.

has been previously reported in response to steroid hormones (Nye et al. 2002; Garcia-Becerra et al. 2010; Kocanova et al. 2010). Similarly, epigenetic modifications encompassing large domains of the genome have been described to participate in gene silencing and, more recently, gene activation during the process of malignant transformation (Hon et al. 2012). Previous studies on the spatial organization of glucocorticoid response in murine cells showed that the hormonal response was facilitated by a preorganized conformation of the nucleus, particularly by cell type-specific chromatin sites accessible to regulatory factors (Hakim et al. 2011). We postulate that the initial organization of TADs could act as topological constraint for changes in gene expression in response to external cues. The transient changes of gene expression in differentiated cells would be constrained by the chromatin state and 3D structure of TADs, which modulates access to genomic sequences for remodeling machineries as well as for specific and general transcription factors (Yadon et al. 2013). Although similar boundaries demarcate TADs before and after Pg stimulation, our analysis demonstrates that the internal organization of TADs is modified upon hormonal stimulation. Indeed, TADs appear to restructure internally after Pg induction. Overall, Pg-induced structural changes were coherently correlated to the epigenetic modifications of the chromatin landscape detected at the TAD scale. Therefore, our results indicate the existence of a link between dynamic structural changes, epigenetic markers, and transcriptional regulation upon transient stimulation in differentiated cells.

Although the molecular mechanisms coordinating the Pg-induced chromatin changes within TADs remain to be fully elucidated, our data suggest that the displacement of H1.2, which has been previously associated with cooperative decondensation of chromatin (Buttinelli et al. 1999; Routh et al. 2008), could participate in those structural transitions by making the chromatin fiber more flexible within activated TADs. As a consequence, TADs activated upon Pg treatment might acquire a more open conformation that could facilitate the recruitment of general transcription machinery and/or the engagement of new regulatory contacts, as suggested by the increase of medium distance interactions. TADs that are transcriptionally repressed upon Pg treatment transition to a more compacted structure, reflected by the facilitated detection of long-range interactions; such changes might limit the accessibility to regulatory proteins. Further analysis with higher coverage and resolution is required to precisely map these changes in specific intra-TAD interactions between regulatory elements and confirm this model (Fig. 5D). Our preliminary single-cell FISH analysis did not show significant differences between the TAD structures prior to and after hormone treatment (Supplemental Fig. 7F,G). High-resolution single-cell experiments therefore will be preferred to properly determine the nature of those predicted structural changes and quantify their frequency of occurrence within the cell population.

In summary, our analysis suggests that specialized TADs respond coordinately upon transient hormonal

stimulation. Importantly, an opposite structural reorganization is observed within activated and repressed TADs. In addition, TADs could respond differentially to distinct hormones. We thus propose that TADs could be considered as units of integration of the numerous pathways that are regulated upon environmental changes. Higher-resolution analysis will be required to determine the variety of changes in the interactions between promoters and enhancers within individual TADs exhibiting an opposite response to hormones. Moreover, whether inter-TAD interactions and nuclear localization modulate the response of individual TADs will have to be elucidated.

## Materials and methods

### *Cell culture and hormonal stimulation*

All experiments (including ChIP-seq, Hi-C, and other high-throughput analyses described in this study) were performed with the following conditions of culture and treatments: T47D cells were grown 48 h in RPMI supplemented with 10% charcoal-treated FBS and synchronized in G0/G1 by 16 h of serum starvation. The Pg analog R5020 or E2 was added to the medium at  $10^{-8}$  M, and cells were harvested after the times indicated.

### *Epigenetic data collection and analysis*

MNase-seq (MNase sequencing), DNase I-seq (DNase I sequencing), and ChIP-seq experiments for H3K4me1, H3K4me3, H2A, H4, RNA polymerase II, PR, H3K9me3, and dHP1 $\gamma$  in T47D cells were described previously (Ballare et al. 2013; Vicent et al. 2013). ChIP-seq experiments for CTCF, H3K36me2, H3K27me3, H3K14ac, and H1.2 were performed under similar conditions using the following antibodies: 07-729 (Millipore), 07-369 (Millipore), 39155 (Active Motif), 07-353 (Millipore), and ab4086 (Abcam), respectively (the number of reads used in this study are summarized in Supplemental Table 2). Reads were processed by aligning to the reference human genome (GRCh37/hg19). MNase-seq, DNase I-seq, and ChIP-seq signals, normalized for sequencing depth, were summed according to different window sizes (ranging from 100 kb to whole TADs). Summed reads were divided by the corresponding signal obtained for an input DNA to determine the normalized signal over input enrichment or depletion. Similarly, Pg-induced enrichment or depletion of mark content was determined for 100-kb bins or the whole TAD as the ratio of sequencing depth-normalized read counts before and after treatment.

### *RNA-seq*

RNA-seq experiments were performed in T47D treated or not with  $10^{-8}$  M R5020 (Pg) for 1 or 6 h or with  $10^{-8}$  M E2 for 6 h. Paired-end reads were mapped with the GEM mRNA Mapping Pipeline (version 1.7) (Marco-Sola et al. 2012) using the latest GENCODE annotation version (version 18) (the number of fragments mapped in the four conditions of culture are summarized in Supplemental Table 3; Harrow et al. 2012). Exon quantifications summarized per gene for expression level determination were obtained as either normalized read counts or reads per kilobase per million mapped reads (RPKM) using a flux capacitor (Montgomery et al. 2010). FCs were computed as the  $\log_2$  ratio of normalized reads per gene obtained after and before treatment with hormones. Genes with FC  $\pm 1.5$  ( $P$ -value  $< 0.05$ ; FDR  $< 0.01$ ) were considered as significantly regulated.

### Generation of contact matrices and integrative modeling of spatial contacts

Hi-C libraries were generated from T47D cells treated or not with R5020 for 60 min according to the previously published Hi-C protocol with minor adaptations (Lieberman-Aiden et al. 2009). Libraries were generated independently in both conditions using HindIII and NcoI restriction enzymes. Hi-C libraries were controlled for quality and sequenced on an Illumina HiSeq 2000 sequencer. Illumina HiSeq paired-end reads were processed by aligning to the reference human genome (GRCh37/hg19) using BWA. Data sets normalized for sequencing depth and experimental biases were used to generate contact matrices at 20, 40, and 100 kb as well as at 1-Mb resolutions (Imakaev et al. 2012).

### Classification of TADs according to their transcriptional response to Pg

To classify TADs according to their hormone response, we calculated the average ratio of the number of normalized RNA-seq reads obtained after and before hormone treatment in the RNA-seq replicates over the whole TAD. TADs containing more than three protein-coding genes were conserved for further analysis and ranked according to the average ratio described above. The top and bottom 100 TADs were classified as “activated” and “repressed,” respectively. To test the homogeneous transcriptional response within the TADs, we calculated the ratio per TAD using, independently, the RNA-seq reads corresponding to either only protein-coding genes or noncoding transcripts detected in the TAD.

### 3D modeling of genomic domains based on Hi-C data

Hi-C produces two-dimensional matrices that represent the frequency of interactions between loci along the genome. To transform such data into a 3D conformation of higher-order chromatin folding, we used the IMP (<http://www.integrativemodeling.org>; Russel et al. 2012). Structure determination by the IMP can be seen as an iterative series of four main steps: generating experimental data, translating the data into spatial restraints, constructing an ensemble of structures that satisfy these restraints, and analyzing the ensemble to produce the final structure. All 3D models were built as previously described (Bau and Marti-Renom 2012).

See the Supplemental Material for further details and additional methods and procedures.

### Data access

Data sets used in this study can be accessed at Gene Expression Omnibus (accession, GSE53463; <http://www.ncbi.nlm.nih.gov/geo/query/acc.cgi?token=kdgbgoucpzurtyh&acc=GSE53463>).

### Acknowledgments

We thank the Centre de Regulació Genòmica (CRG) Ultrasequencing Unit and Advanced Light Microscopy Unit for technical support, and all members of the Chromatin and Gene Expression and Structural Genomic groups for helpful discussions. We acknowledge Juan Valcarcel for his helpful comments on the manuscript. We also thank Marta Morell and the Genetic Causes of Disease group for providing the BAC clones used in this study. We thank Ivan Junier for his help and advice in normalizing the Hi-C data. We acknowledge financial support from the Spanish Ministry of Economy and Competitiveness (MINECO) (BFU2010-19310/BMC) and the Human Frontiers Science Program (RGP0044/2011) (to M.A.M.-R.). This work was also supported by grants from the

Spanish government (BMC 2003-02902, BMC 2010-15313, and CSD2006-00049) and the Catalan government (Agència de Gestió d'Ajuts Universitaris i de Recerca [AGAUR]) (to M.B.). We acknowledge support of the Spanish Ministry of Economy and Competitiveness, ‘Centro de Excelencia Severo Ochoa 2013-2017,’ SEV-2012-0208. F.L.D., G.F., M.A.M.-R., and M.B. designed the studies. F.L.D. performed Hi-C, FISH, and RNA-seq experiments. G.V., R.H.G.W., and C.B. performed ChIP-seq experiments. F.L.D. carried out the data analysis with contributions from A.P., D.S., G.C., and G.F., and F.S., D.B., and M.A.M.-R. carried out the 3D modelling and analysis. F.S. and G.F. designed the TAD boundary algorithm. All of the authors discussed the results, and F.L.D., M.A.M.-R., and M.B. wrote the manuscript.

### References

- Ballare C, Castellano G, Gaveglia L, Althammer S, Gonzalez-Vallinas J, Eyras E, Le Dily F, Zaurin R, Soronellas D, Vicent GP, et al. 2013. Nucleosome-driven transcription factor binding and gene regulation. *Mol Cell* **49**: 67–79.
- Bau D, Marti-Renom MA. 2012. Genome structure determination via 3C-based data integration by the integrative modeling platform. *Methods* **58**: 300–306.
- Bau D, Sanyal A, Lajoie BR, Capriotti E, Byron M, Lawrence JB, Dekker J, Marti-Renom MA. 2011. The three-dimensional folding of the  $\alpha$ -globin gene domain reveals formation of chromatin globules. *Nat Struct Mol Biol* **18**: 107–114.
- Buttinelli M, Panetta G, Rhodes D, Travers A. 1999. The role of histone H1 in chromatin condensation and transcriptional repression. *Genetica* **106**: 117–124.
- Caron H, van Schaik B, van der Mee M, Baas F, Riggins G, van Sluis P, Hermus MC, van Asperen R, Boon K, Voute PA, et al. 2001. The human transcriptome map: clustering of highly expressed genes in chromosomal domains. *Science* **291**: 1289–1292.
- Cavalli G. 2007. Chromosome kissing. *Curr Opin Genet Dev* **17**: 443–450.
- Dekker J, Rippe K, Dekker M, Kleckner N. 2002. Capturing chromosome conformation. *Science* **295**: 1306–1311.
- Dekker J, Marti-Renom MA, Mirny LA. 2013. Exploring the three-dimensional organization of genomes: interpreting chromatin interaction data. *Nat Rev Genet* **14**: 390–403.
- Dixon JR, Selvaraj S, Yue F, Kim A, Li Y, Shen Y, Hu M, Liu JS, Ren B. 2012. Topological domains in mammalian genomes identified by analysis of chromatin interactions. *Nature* **485**: 376–380.
- Dostie J, Richmond TA, Arnaout RA, Selzer RR, Lee WL, Honan TA, Rubio ED, Krumm A, Lamb J, Nusbaum C, et al. 2006. Chromosome conformation capture carbon copy (5C): a massively parallel solution for mapping interactions between genomic elements. *Genome Res* **16**: 1299–1309.
- Fullwood MJ, Liu MH, Pan YF, Liu J, Xu H, Mohamed YB, Orlov YL, Velkov S, Ho A, Mei PH, et al. 2009. An oestrogen-receptor- $\alpha$ -bound human chromatin interactome. *Nature* **462**: 58–64.
- Garcia-Becerra R, Berno V, Ordaz-Rosado D, Sharp ZD, Cooney AJ, Mancini MA, Larrea F. 2010. Ligand-induced large-scale chromatin dynamics as a biosensor for the detection of estrogen receptor subtype selective ligands. *Gene* **458**: 37–44.
- Hakim O, Sung MH, Voss TC, Splinter E, John S, Sabo PJ, Thurman RE, Stamatoyannopoulos JA, de Laat W, Hager GL. 2011. Diverse gene reprogramming events occur in the same spatial clusters of distal regulatory elements. *Genome Res* **21**: 697–706.
- Harrow J, Frankish A, Gonzalez JM, Tapanari E, Diekhans M, Kokocinski F, Aken BL, Barrell D, Zadis A, Searle S, et al.

Le Dily et al.

2012. GENCODE: the reference human genome annotation for The ENCODE Project. *Genome Res* **22**: 1760–1774.
- Hon GC, Hawkins RD, Caballero OL, Lo C, Lister R, Pelizzola M, Valsesia A, Ye Z, Kuan S, Edsall LE, et al. 2012. Global DNA hypomethylation coupled to repressive chromatin domain formation and gene silencing in breast cancer. *Genome Res* **22**: 246–258.
- Hou C, Li L, Qin ZS, Corces VG. 2012. Gene density, transcription, and insulators contribute to the partition of the *Drosophila* genome into physical domains. *Mol Cell* **48**: 471–484.
- Imakaev M, Fudenberg G, McCord RP, Naumova N, Goloborodko A, Lajoie BR, Dekker J, Mirny LA. 2012. Iterative correction of Hi-C data reveals hallmarks of chromosome organization. *Nat Methods* **9**: 999–1003.
- Jin F, Li Y, Dixon JR, Selvaraj S, Ye Z, Lee AY, Yen CA, Schmitt AD, Espinoza CA, Ren B. 2013. A high-resolution map of the three-dimensional chromatin interactome in human cells. *Nature* **503**: 290–294.
- Kalhor R, Tjong H, Jayathilaka N, Alber F, Chen L. 2012. Genome architectures revealed by tethered chromosome conformation capture and population-based modeling. *Nat Biotechnol* **30**: 90–98.
- Kocanova S, Kerr EA, Rafique S, Boyle S, Katz E, Caze-Subra S, Bickmore WA, Bystricky K. 2010. Activation of estrogen-responsive genes does not require their nuclear co-localization. *PLoS Genet* **6**: e1000922.
- Lieberman-Aiden E, van Berkum NL, Williams L, Imakaev M, Ragoczy T, Telling A, Amit I, Lajoie BR, Sabo PJ, Dorschner MO, et al. 2009. Comprehensive mapping of long-range interactions reveals folding principles of the human genome. *Science* **326**: 289–293.
- Marco-Sola S, Sammeth M, Guigo R, Ribeca P. 2012. The GEM mapper: fast, accurate and versatile alignment by filtration. *Nat Methods* **9**: 1185–1188.
- Mateos-Langerak J, Bohn M, de Leeuw W, Giromus O, Manders EM, Verschure PJ, Indemans MH, Gierman HJ, Heermann DW, van Driel R, et al. 2009. Spatially confined folding of chromatin in the interphase nucleus. *Proc Natl Acad Sci* **106**: 3812–3817.
- Migliaccio A, Piccolo D, Castoria G, Di Domenico M, Bilancio A, Lombardi M, Gong W, Beato M, Auricchio F. 1998. Activation of the Src/p21ras/Erk pathway by progesterone receptor via cross-talk with estrogen receptor. *EMBO J* **17**: 2008–2018.
- Montgomery SB, Sammeth M, Gutierrez-Arcelus M, Lach RP, Ingle C, Nisbett J, Guigo R, Dermitzakis ET. 2010. Transcriptome genetics using second generation sequencing in a Caucasian population. *Nature* **464**: 773–777.
- Nora EP, Lajoie BR, Schulz EG, Giorgetti L, Okamoto I, Servant N, Piolot T, van Berkum NL, Meisig J, Sedat J, et al. 2012. Spatial partitioning of the regulatory landscape of the X-inactivation centre. *Nature* **485**: 381–385.
- Nora EP, Dekker J, Heard E. 2013. Segmental folding of chromosomes: a basis for structural and regulatory chromosomal neighborhoods? *BioEssays* **35**: 818–828.
- Nye AC, Rajendran RR, Stenoien DL, Mancini MA, Katzenellenbogen BS, Belmont AS. 2002. Alteration of large-scale chromatin structure by estrogen receptor. *Mol Cell Biol* **22**: 3437–3449.
- Osborne CS, Chakalova L, Brown KE, Carter D, Horton A, Debrand E, Goyenechea B, Mitchell JA, Lopes S, Reik W, et al. 2004. Active genes dynamically colocalize to shared sites of ongoing transcription. *Nat Genet* **36**: 1065–1071.
- Osborne CS, Chakalova L, Mitchell JA, Horton A, Wood AL, Bolland DJ, Corcoran AE, Fraser P. 2007. Myc dynamically and preferentially relocates to a transcription factory occupied by Igh. *PLoS Biol* **5**: e192.
- Routh A, Sandin S, Rhodes D. 2008. Nucleosome repeat length and linker histone stoichiometry determine chromatin fiber structure. *Proc Natl Acad Sci* **105**: 8872–8877.
- Russel D, Lasker K, Webb B, Velazquez-Muriel J, Tjioe E, Schneidman-Duhovny D, Peterson B, Sali A. 2012. Putting the pieces together: integrative modeling platform software for structure determination of macromolecular assemblies. *PLoS Biol* **10**: e1001244.
- Sanyal A, Lajoie BR, Jain G, Dekker J. 2012. The long-range interaction landscape of gene promoters. *Nature* **489**: 109–113.
- Sexton T, Yaffe E, Kenigsberg E, Bantignies F, Leblanc B, Hoichman M, Parrinello H, Tanay A, Cavalli G. 2012. Three-dimensional folding and functional organization principles of the *Drosophila* genome. *Cell* **148**: 458–472.
- Shen Y, Yue F, McCleary DF, Ye Z, Edsall L, Kuan S, Wagner U, Dixon J, Lee L, Lobanenkov VV, et al. 2012. A map of the cis-regulatory sequences in the mouse genome. *Nature* **488**: 116–120.
- Symmons O, Uslu VV, Tsujimura T, Ruf S, Nassari S, Schwarzer W, Ettwiller L, Spitz F. 2014. Functional and topological characteristics of mammalian regulatory domains. *Genome Res* **24**: 390–400.
- Thurman RE, Rynes E, Humbert R, Vierstra J, Maurano MT, Haugen E, Sheffield NC, Stergachis AB, Wang H, Vernot B, et al. 2012. The accessible chromatin landscape of the human genome. *Nature* **489**: 75–82.
- Truss M, Bartsch J, Schelbert A, Hache RJ, Beato M. 1995. Hormone induces binding of receptors and transcription factors to a rearranged nucleosome on the MMTV promoter in vivo. *EMBO J* **14**: 1737–1751.
- Vicent GP, Ballare C, Nacht AS, Clausell J, Subtil-Rodriguez A, Quiles I, Jordan A, Beato M. 2006. Induction of progesterone target genes requires activation of Erk and Msk kinases and phosphorylation of histone H3. *Mol Cell* **24**: 367–381.
- Vicent GP, Ballare C, Nacht AS, Clausell J, Subtil-Rodriguez A, Quiles I, Jordan A, Beato M. 2008. Convergence on chromatin of non-genomic and genomic pathways of hormone signaling. *J Steroid Biochem Mol Biol* **109**: 344–349.
- Vicent GP, Nacht AS, Font-Mateu J, Castellano G, Gaveglia L, Ballare C, Beato M. 2011. Four enzymes cooperate to displace histone H1 during the first minute of hormonal gene activation. *Genes Dev* **25**: 845–862.
- Vicent GP, Nacht AS, Zaurin R, Font-Mateu J, Soronellas D, Le Dily F, Reyes D, Beato M. 2013. Unliganded progesterone receptor-mediated targeting of an RNA-containing repressive complex silences a subset of hormone-inducible genes. *Genes Dev* **27**: 1179–1197.
- Wright RH, Castellano G, Bonet J, Le Dily F, Font-Mateu J, Ballare C, Nacht AS, Soronellas D, Oliva B, Beato M. 2012. CDK2-dependent activation of PARP-1 is required for hormonal gene regulation in breast cancer cells. *Genes Dev* **26**: 1972–1983.
- Yadon AN, Singh BN, Hampsey M, Tsukiyama T. 2013. DNA looping facilitates targeting of a chromatin remodeling enzyme. *Mol Cell* **50**: 93–103.
- Yaffe E, Tanay A. 2011. Probabilistic modeling of Hi-C contact maps eliminates systematic biases to characterize global chromosomal architecture. *Nat Genet* **43**: 1059–1065.